



## Housing and Building National Research Center HBRC Journal

<http://ees.elsevier.com/hbrcj>



# Damage detection of plate-like structures based on residual force vector



Atef Eraky <sup>a</sup>, Alaa Saad <sup>a</sup>, Ahmed M. Anwar <sup>b</sup>, Ayman Abdo <sup>a,\*</sup>

<sup>a</sup> Structural Eng. Dep., Faculty of Engineering, Zagazig University, Egypt

<sup>b</sup> Construction Research Institute, National Water Research Center, Egypt

Received 5 June 2014; revised 7 January 2015; accepted 8 January 2015

### KEYWORDS

Damage detection;  
Plate structures;  
MatLab;  
Residual force vector

**Abstract** Structural health monitoring is essential to maintain the structural integrity by predicting problems in an early time. This consequently could be reflected on extending the life time of structures. Nondestructive tests based on dynamic measures are usually fast and economic in detecting damages of structures. Various numerical techniques together with recording time histories are used for this purpose. This paper presents a numerical method for damage detection in plate-like structures. The modeling of damage was conducted commercially using the module of MatLab. Comparison of different mode shapes was used in the analysis to detect the location of local damage based on residual force vector. The technique utilized the node residual force vector to locate and evaluate the degree of the suspected damaged elements. In the current study, three configurations for plates were used. The study also concentrated on the efficiency of the new method in identifying damages of different degradation levels. The plates were subjected to different combinations of artificial damages applied at various positions on each plate. The study was not only able to identify the location but also the degree of damage in plates. It has been noted that identification of severe degradation was more precisely identified. As a result, the residual force method is the simplest damage quantification technique which approved to be accurate enough to be used in practical applications.

© 2015 The Authors. Production and hosting by Elsevier B.V. on behalf of Housing and Building National Research Center. This is an open access article under the CC BY-NC-ND license (<http://creativecommons.org/licenses/by-nc-nd/4.0/>).

### Introduction

Accumulation of damage among structure can cause severe structural failure. Development of an early damage detection method for structural failure is one of the most important keys in maintaining the integrity and safety of structures. The dynamics-based damage detection is an effective method due to its simplicity of implementation and ability of acquiring both global and local information of structure. Significant efforts have already been spent to develop damage detection algorithms using dynamics-based approach [1].

\* Corresponding author.

Peer review under responsibility of Housing and Building National Research Center.



Production and hosting by Elsevier

Techniques based on dynamic parameters for detecting damages in a structure have attracted much attention in recent years. Modal frequencies and mode shapes are the most popular parameters used in damage identification. The basic idea of these techniques is that modal parameters are functions of physical properties of structure (mass, damping and stiffness). Therefore, changes in physical properties will cause changes in modal properties. Many methods were developed recently using modal parameters as damage indicators.

An important class of damage identification methods is based on the updating or modification of structural matrices. The residual force vector is widely used in many damage detection methods using optimal matrix modification. Chen et al. [2] put forward a theory for assessing the occurrence, location and extent of potential damage using on-orbit response measurements. This method detects damages by using the minimum norm solution of the residual force equation. Zimmerman et al. [3] made use of a minimum rank update theory to detect structural damages. The damage sites are located firstly by the residual force vector and the damage extents are assessed by the minimum rank update theory. Doebling [4] improved this method and presented a new technique termed the minimum-rank elemental update by computing the minimum rank updates directly to the elemental stiffness parameters, Leandro et al. [5] and Damir et al. [6]. Chiang et al. [7] presented a two-stage structural damage detection method. The residual force vector is used to localize damages preliminarily and the simulated evolution method is employed to determine damage extents. Mares and Surace [8] proposed a genetic algorithm to identify damage in elastic structures. The location and quantification of the extent of the damage is performed with genetic techniques implemented by using the residual force method, which is based on conventional modal analysis theory. In short, these above methods all begin with the residual force vector but use different techniques to obtain damage extents, so the accuracy of the residual force vector is very important to those methods. The minimum norm method is shown to be unfeasible in damage identification in practice because the residual force equation is ill conditioned with the measurement noises, while the minimum rank update techniques can obtain better results only when the number of modes used in calculation equals the rank of perturbed matrix. Ratcliffe [9] develops and presents the Laplacian operator on the mode shapes to locate damage. When the damage is severe, the results are successful. For minor damages a further processing of the Laplacian output is required. The procedure operates solely on the mode shape from the damaged structure, and does not require a priori knowledge of the undamaged structure.

Pandey et al. [10] employed the change in the mode shapes curvature to detect damage. The curvatures are obtained using a central difference approximation. Hajela and Soeiro [11] studied structural damage detection based on static and modal analysis. Chakraverty et al. [12] and Leandro et al. [13] have been studied the effect of non-homogeneity and different parameters on natural frequencies of vibration for plate damage detection. In a situation with little displacements, the curvature approximation becomes very sensitive to the presence of noise. Identifying the structural damage with the measured vibration data is an inverse approach in mathematics. The usual damage detection methods minimize an objective function, which is defined in terms of the discrepancies between the vibration data identified by modal testing and those computed from

the analytical model. Titurus et al. [14] discussed damage detection using successive parameter subset selections and multiple modal residuals.

The purpose of this work is to use the residual force method in order to detect structural damages successfully in plate structures. Also, to verify the efficiency of the developed technique on different structures with different damage ratios. Computer program using MatLab is employed to find out the location and extent of the damage.

## Theory and modeling

### Numerical simulation

The equation of motion of the structure when subjected to dynamic loads is:

$$M\ddot{y} + C\dot{y} + Ky = F \quad (1)$$

where  $M$ ,  $C$ , and  $K$  are the mass, damping and stiffness matrices of the structure, respectively.  $\ddot{y}$ ,  $\dot{y}$ , and  $y$  are the acceleration, velocity and displacement vectors of the structure, respectively.  $F$  is the dynamic force. The mass and stiffness matrices of the structure are computed by the assembly of mass and stiffness matrices of the structure elements. In this section, the global stiffness and mass matrices in case of plate elements will be derived.

The plane stress equations can be used to relate the in-plane stresses to the in-plane strains for an isotropic material as:

$$\sigma_x = \frac{E}{1 - \nu^2} (\epsilon_x + \nu \cdot \epsilon_y) \quad (2)$$

$$\sigma_y = \frac{E}{1 - \nu^2} (\epsilon_y + \nu \cdot \epsilon_x) \quad (3)$$

$$\tau_{xy} = G\gamma_{xy} \quad (4)$$

where  $\sigma_x$  and  $\sigma_y$  are the normal stress in  $X$  and  $Y$  directions, respectively.  $\tau_{xy}$  is the shear stress acts on the  $X$  edge (vertical face) in the  $Y$ -direction.

Fig. 1 shows the plate structure model and the schematic diagram of four nodes plate. Each node has three degrees of freedom – transverse displacement  $w$  in the  $Z$ -direction, rotation  $\theta_x$  about the  $X$ -axis, and rotation  $\theta_y$  about the  $Y$ -axis.

The nodal displacements at node  $i$  can be presented by [15]:

$$\{d\} = \begin{Bmatrix} w_i \\ \theta_{xi} \\ \theta_{yi} \end{Bmatrix} \quad (5)$$

where the rotations are correlated to the transversal displacements by:

$$\theta_x = +\frac{\partial w}{\partial y}, \quad \theta_y = -\frac{\partial w}{\partial x} \quad (6)$$

The negative sign of  $\theta_y$  is due to the fact that a negative displacement  $w$  is required to produce a positive rotation about the  $Y$ -axis.

The total element displacement matrix is now given by:

$$\{d\} = \{d_i \quad d_j \quad d_m \quad d_n\}^T \quad (7a)$$

The constants  $a_1$  through  $a_{12}$  can be determined by expressing the 12 simultaneous equations linking the values of  $w$  and its slopes at the nodes when the coordinates take up their appropriate values.

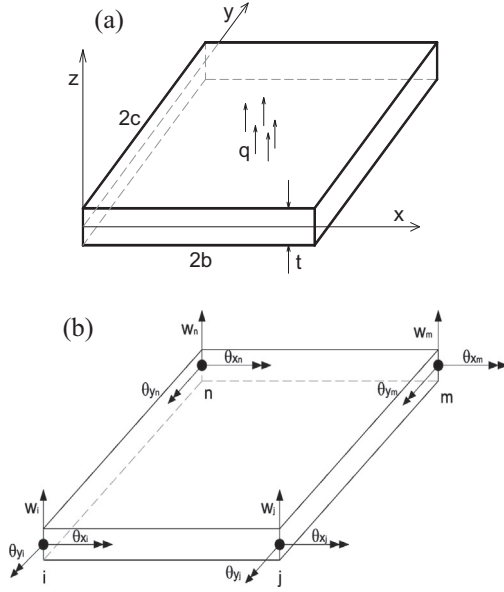


**Fig. 1** (a) Four nodes plate structure model. (b) Schematic diagram of the 12 plate nodal DOFs.

$$\left\{ \begin{matrix} \omega \\ +\frac{\partial \omega}{\partial y} \\ -\frac{\partial \omega}{\partial x} \end{matrix} \right\} = \begin{bmatrix} 1 & x & y & x^2 & xy & y^2 & x^3 & x^2y & xy^2 & y^3 & x^3y & xy^3 \\ 0 & 0 & 1 & 0 & x & 2y & 0 & x^2 & 2xy & 3y^2 & x^3 & 3xy^2 \\ 0 & -1 & 0 & -2x & -y & 0 & 2x^2 & -2xy & -y^2 & 0 & -2x^2y & -y^2 \end{bmatrix} \begin{Bmatrix} a_1 \\ a_2 \\ a_{12} \end{Bmatrix} \quad (7b)$$

or in this form

$$\{d\} = [C_o]\{a\} \quad (8)$$

By defining the strain (curvature)/displacement and stress (-moment)/curvature relationships

$$k_x = \frac{\partial^2 w}{\partial x^2}, \quad k_y = \frac{\partial^2 w}{\partial y^2}, \quad k_{xy} = \frac{2\partial^2 w}{\partial x \partial y} \quad (9)$$

$$\begin{Bmatrix} k_x \\ k_y \\ k_{xy} \end{Bmatrix} = \begin{Bmatrix} -2a_4 - 6a_7x - 2a_8y - 6a_{11}xy \\ -2a_6 - 2a_9x - 6a_{10}y - 6a_{12}xy \\ -2a_5 - 4a_8x - 4a_9y - 6a_{11}x^2 - 6a_{12}y^2 \end{Bmatrix} \quad (10)$$

or in matrix form as:

$$\{k\} = \{Q\}\{a\} \quad (11)$$

The  $[D]$  matrix is the constitutive matrix given for isotropic materials and given by:

$$D = \frac{Et^3}{12(1-\nu^2)} \begin{bmatrix} 1 & \nu & 0 \\ \nu & 1 & 0 \\ 0 & 0 & \frac{1-\nu}{2} \end{bmatrix} \quad (12)$$

where  $E$  is modulus of elasticity,  $t$  is the plate element thickness, and  $\nu$  is the poisson ratio.

Then the stiffness matrix can be constructed to the four nodes plate element using general relation as follows:

$$[K] = [B]^T[D][B]dV \quad (13)$$

$$\text{where } [B] = [Q][C_o]^{-1} \quad (14)$$

In this case, the differential volume element  $dV = tdx dy$  and the integral is over the range  $x = -b$  to  $+b$  and  $y = -c$  to  $+c$ . Hence, in non-dimensional coordinates,  $dV = abt d\xi d\eta$  and

integration is over the range  $\xi = -1$  to  $+1$  and  $\eta = -1$  to  $+1$ . And  $Q$  is the coefficient matrix. The stiffness matrix then becomes

$$[k] = abt \int_{-1}^{+1} \int_{-1}^{+1} [B]^T[D][B]d\xi d\eta \quad (15)$$

The global mass matrix of plate element is derived as

$$[M]_e = \rho h \int [N]^T[N] dA \quad (16)$$

where  $\rho$  is the mass density of a material,  $N$  is the shape (interpolation or basis) function matrix. The element stiffness and mass matrices are assembled to get global matrices.

#### Formulation of damage detection technique using residual force vector

Assuming that the mass matrix is unchangeable and is not affected by the presence of damage; the Eigen value equation for  $n$  Dofs model of a damaged structure is [10]:

$$(K_d - \lambda_{dj}M)\phi_{dj} = 0 \quad (17)$$

where  $M$  is the structure mass matrix,  $K_d$  is the stiffness matrix associated with the damaged structural model,  $\lambda_{dj}$  and  $\phi_{dj}$  are the  $j$ th eigenvalue and eigenvector of the damaged structure, respectively, which are obtained from the system identification procedure or directly from field using modern instruments such as scanning laser vibrometer.

The damaged structural stiffness matrix is calculated as follows:

$$K_d = K - \Delta K \quad (18)$$

where  $K_u$  is the undamaged structure stiffness matrix and  $\Delta K$  is the corresponding changes in the stiffness matrix.

Substituting Eq. (18) into Eq. (17) yields [16]:

$$\Delta K \phi_{dj} = (K - \lambda_{dj} M) \phi_{dj} \quad (19)$$

$$\Delta K \phi_{dj} = b_j \quad (20)$$

then Eq. (19) can be rewritten as:

$$b_j = (K - \lambda_{dj} M) \phi_{dj} \quad (21)$$

where  $b_j$  is the  $j$ th residual force vector.

Eq. (20) can be expressed as:

$$\begin{bmatrix} \Delta k_1^T \\ \Delta k_2^T \\ \vdots \\ \Delta k_n^T \end{bmatrix} * \phi_{dj} = \begin{Bmatrix} b_{j1} \\ b_{j2} \\ \vdots \\ b_{jn} \end{Bmatrix} \quad (22)$$

A residual force square matrix  $R$  is formed with size  $(n \times n)$  as  $n$  is the number of degrees of freedom, where each column in this matrix presents the vector  $(b_j)$  as follows:

$$R = [b_1 \quad b_2 \quad \dots \quad b_j \quad \dots \quad b_n] \quad (23)$$

The residual force matrix  $R$  is reshaped to be a single vector with size  $(n^2 \times 1)$  called the reshaped residual force  $R^*$ :

$$R^* = [b_1 \quad b_2 \quad b_3 \quad b_4 \dots b_j \dots b_n]^T \quad (24)$$

Damaged modal stiffness matrix ( $E$ ) has to be constructed by the following steps [17]:

1. The global stiffness matrix of each element of the undamaged structure ( $k_i^g$ ) is constructed as in Eq. (15).
2. Each element stiffness matrix is reduced by eliminating the restrained degrees of freedom and the reduced matrix ( $k_i^r$ ) is multiplied by rows of damage modal matrix  $\phi_d$  that corresponding to degrees of freedom associated with element ones. The matrix resulted from multiplication called  $k_\phi$ .
3. A Square matrix ( $k_{nn}$ ) with size ( $n \times n$ ) is filled with matrix  $k_\phi$  so that all elements of matrix ( $k_{nn}$ ) are zeros except the items that corresponding to the associated element degrees of freedom filled with the matrix ( $k_\phi$ ).
4. The matrix  $k_{nn}$  is reshaped to be one column with size ( $n^2 \times 1$ ) called  $k_{nn}^{ast}$ .
5. The matrix  $k_{nn}^*$  is assembled in a matrix  $E$  with size ( $n^2 \times n_e$ ), where  $n_e$  is number of elements, so that the matrix  $k_{nn}^*$  is placed in the  $i$ th column of the matrix  $E$  where  $i$  is the element number.
6. Repeat the previous steps for each element to fill the matrix  $E$ .

The relation between the reshaped residual force vector  $R^*$  and the matrix  $E$  is as follows:

$$E\alpha = R^* \quad (25)$$

where  $\alpha$  is the damage ratios vector which contains the damage ratio in each element of the structure ( $\alpha_i$ ) as follows:

$$\alpha = [\alpha_1 \quad \alpha_2 \quad \alpha_3 \dots \alpha_{ne}]^T \quad (26)$$

where  $ne$  represents the number of elements. The element damage ratios can be then obtained as follows:

$$\alpha = E^+ R^* \quad (27)$$

where  $E^+$  is the pseudo-inverse of the matrix  $E$ .

#### Mode shape expansion

The most popular and simplest method was introduced by Guyan [18]. State and force vectors,  $x$  and  $f$ , and Mass and stiffness matrices,  $M$  and  $K$ , are split into subvectors and submatrices relating to the retained master degrees of freedom which are transitions and the eliminated slave degrees of freedom which are rotations. If no force is applied to the slave degrees of freedom, one can obtain [19]:

$$\begin{bmatrix} [M_{mm}] & [M_{ms}] \\ [M_{sm}] & [M_{ss}] \end{bmatrix} \begin{Bmatrix} \ddot{x}_m \\ \ddot{x}_s \end{Bmatrix} + \begin{bmatrix} [K_{mm}] & [K_{ms}] \\ [K_{sm}] & [K_{ss}] \end{bmatrix} \begin{Bmatrix} x_m \\ x_s \end{Bmatrix} = \begin{Bmatrix} f_m \\ 0 \end{Bmatrix} \quad (28)$$

The subscripts  $m$  and  $s$  relate to the master and slave coordinates respectively.

Neglecting the inertia terms for the second set of equations it can be obtained:

$$K_{sm}K_m + K_{ss}X_s = 0 \quad (29)$$

which may be used to eliminate the slave degrees of freedom as follows:

$$\begin{bmatrix} x_m \\ x_s \end{bmatrix} = \begin{bmatrix} [I] \\ -[K_{ss}]^{-1}[K_{sm}] \end{bmatrix} x_m = [T_s]x_m \quad (30)$$

where  $[T_s]$  denotes the static transformation between the full state vector and the master co-ordinates, so the expanded mode shapes are:

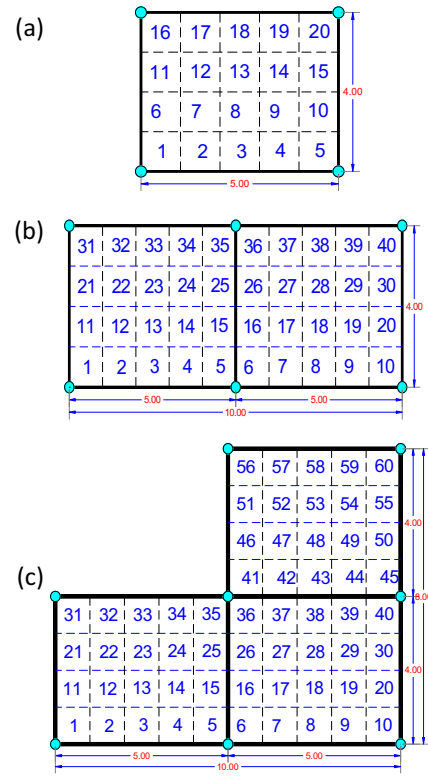


**Fig. 2** Meshing of the plate structure for; (a) 1 bay plate (P1), (b) 2 bays plate (P2), and (c) 3 bays plate (P3).

**Table 1** Properties of the Studied Structures.

Flexural member	Plate (2D)
Statical system	Simply supported
Element type	Plane stress
Material	Concrete
Length	5.0 m
Width	4.0 m
Depth	0.2 m
Poisson's ratio	0.2
Mass density	2.5 t/m <sup>3</sup>
Modulus of elasticity	20 GPa

**Table 2** Damage severity in damaged plate.

Type	Damage (%)	Condition
DA	10	Minor
DB	40	Moderate
DC	90	Severe

$$\begin{bmatrix} \phi_m \\ \phi_s \end{bmatrix} = \begin{bmatrix} [I] \\ -[K_{ss}]^{-1}[K_{sm}] \end{bmatrix} [\phi_m] = [T_s][\phi_m] \quad (31)$$

Notice that the masters' degrees of freedom remain unchanged as seen by the upper partition of this equation:

$$[\phi_m] = [I][\phi_m] \quad (32)$$

and that the deleted DOF are estimated by:

$$[\phi_s] = [-[K_{ss}]^{-1}[K_{sm}]][\phi_m] \quad (33)$$

**Table 3** Different Combinations of Damage.

Model	Combination	DA	DB	DC
Model #1	#1	Element #1	–	–
	#2	Element #1	Element #8	–
	#3	Element #1	Element #8	Element #19
Model #2	#4	Element #1	Element #11	–
	#5	Element #1	Element #11	Element #31
Model #3	#6	Element #1	Element #13	–
	#7	Element #1	Element #13	Element #48

However, since this technique is based on static stiffness of the system, there is no guarantee that the mode shape expansion will be accurate. The Guyan expansion process will not produce acceptable results unless there are sufficient degrees of freedom to describe the mass inertia of the system. If sufficient degrees of freedom are available, then the Guyan process will produce reasonably good results but will never produce exact results since the inherent formulation of the transformation matrix is approximate.

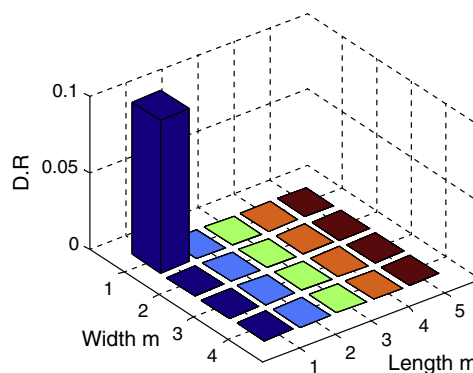
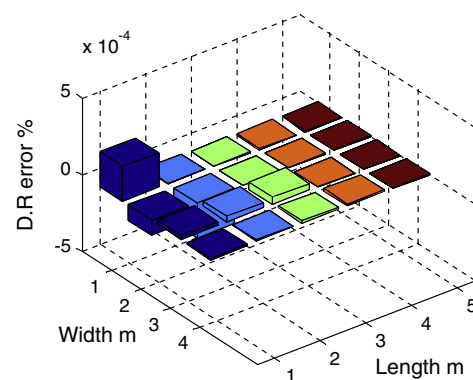
### Synthetic verification

Three different configurations for plates were selected to examine the efficiency of the damage detection self-made module. The first plate (P1) was of dimensions ( $4.0 \times 5.0$  m) and was simply supported in both directions. The second plate assembly (P2) consisted of two continuous plates in the long direction. While the third plate configuration (P3) was for L-shape plate – one central plate similar to that of the first configuration with continuation in two perpendicular directions. All plates were divided into elements of finer size of dimension ( $1.0 \times 1.0$  m). Fig. 2a–c shows the arrangement for the three examined plates, respectively. Table 1 shows the properties of the plate materials and the dimensions of the plate model. In this research, combinations of different degrees of damage were applied in random scenarios for each plate. The damage was simulated by reducing the modulus of Elasticity of the desired element to certain level. The element damage ratio could then be defined as the change in element stiffness. Three levels of damage ratios were studied; 0.1, 0.4 and 0.9 and will be denoted by DA, DB, and DC, respectively, as shown in Table 2. These values are representative of minor, moderate and severe damage, respectively. Seven combinations shown in Table 3 will be discussed in the next part.

### Results and discussion

#### Damage detection of the first model

In the single damaged element scenario, where damage occurred in only one element while the rest of elements were kept in sound state. To check the proposed techniques, an example of small damage, as shown in Fig. 3, where element #1 was damaged slightly (DA). The response of the damaged plate was obtained and used as input to the numerical model which calculated the damage ratio for each element. It was demonstrated that the damage ratio in each element was approximately equal to zero except the element number one

**Fig. 3** Damage ratio for combination #1.**Fig. 4** Damage detection error for combination #1.

which has damage ratio coincided with the occurred damage ratio (0.1). The error in damage detection was calculated as the absolute difference between the detected and the actual damage ratio as a percent in each element.

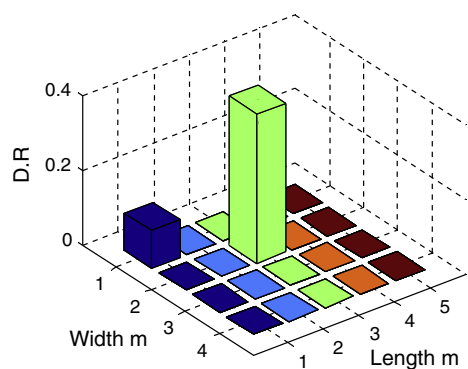
It was found that the error in all elements was very small as shown in Fig. 4, where they obtained maximum absolute error was equal to  $2.3e-4\%$  and occurred in elements #1 and #6. Table 4 lists in detail the results of this case.

Another scenario of making moderate damage, 0.4, (DB) was performed in plate element #8 in addition the slightly damage (DA) in plate element #1. The detected damage ratio in all moderate damage cases is shown in Fig. 5, where a damage ratio equals 0.4 is detected in the assumed damaged



**Table 4** Damage ratio in all members.

Element No.	Damage ratio	Error (%)
1	0.099998	2.25E-05
2	3.01E-08	3.01E-06
3	1.74E-08	1.74E-06
4	-7.34E-08	-7.34E-06
5	-2.60E-08	-2.60E-06
6	-9.75E-07	-9.75E-05
7	-2.30E-06	-2.30E-04
8	1.11E-08	1.11E-06
9	1.95E-08	1.95E-06
10	2.22E-08	2.22E-06
11	2.26E-07	2.26E-05
12	3.33E-07	3.33E-05
13	4.43E-07	4.43E-05
14	-1.55E-08	-1.55E-06
15	5.24E-09	5.24E-07
16	-9.38E-08	-9.38E-06
17	6.06E-08	6.06E-06
18	1.41E-07	1.41E-05
19	1.09E-07	1.09E-05
20	5.24E-09	5.24E-07

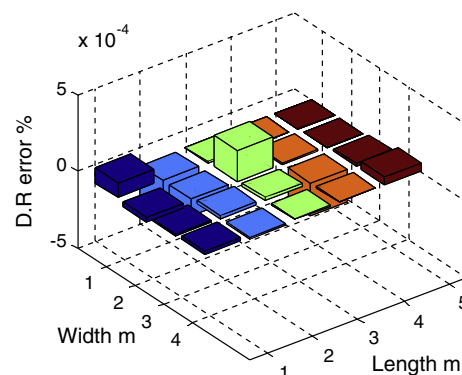
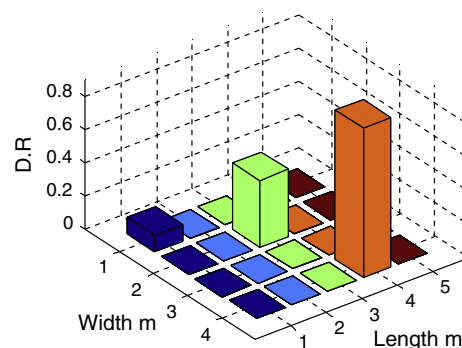
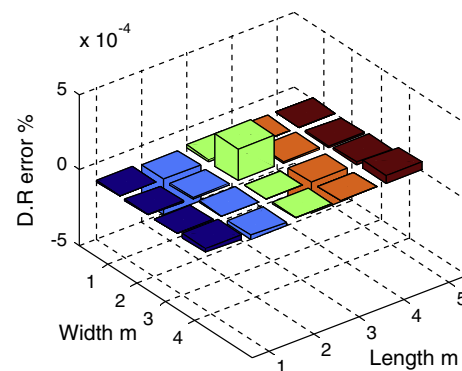
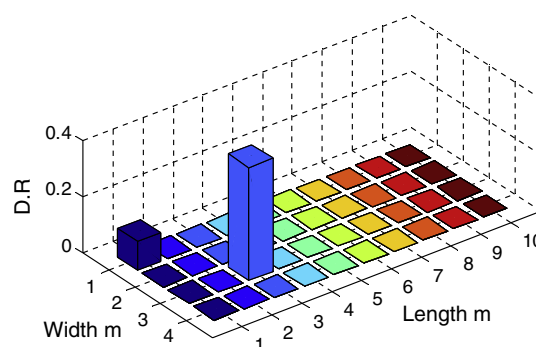
**Fig. 5** Damage ratio for combination #2.

element for each case. The error in detecting damage ratio is represented by bar chart (histogram) as shown in Fig. 6, and the maximum error occurs in element #7 and it was equal to  $2.7\text{e-}4\%$ .

When a severe damage, 0.9, (Dc) is occurred in plate element #19 in addition to the two pointed damage previously, the proposed technique detected the damage ratio as shown in Fig. 7. The error in detecting the damage ratio was very small as shown in Fig. 8, which shows that, the maximum damage detection error equals to  $1.9\text{e-}4\%$ .

#### Damage detection of the second model

The previous technique was applied to the second plate model. Figs. 9 and 11 show the damage ratio of the two cases of damages of model 2. The detected damage ratios of all cases when a small, moderate and sever damages are occurred in each element individually are shown. The error and the maximum error in detecting the damage ratio of each case are shown in

**Fig. 6** Damage detection percentage error for combination #2.**Fig. 7** Damage ratio for combination #3.**Fig. 8** Damage detection error % for combination #3.**Fig. 9** Damage ratio for combination #4.

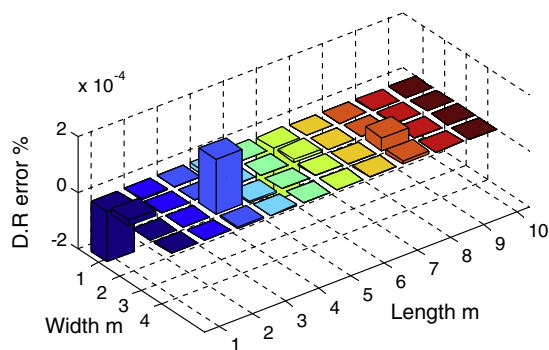


Fig. 10 Damage detection error % for combination #4.

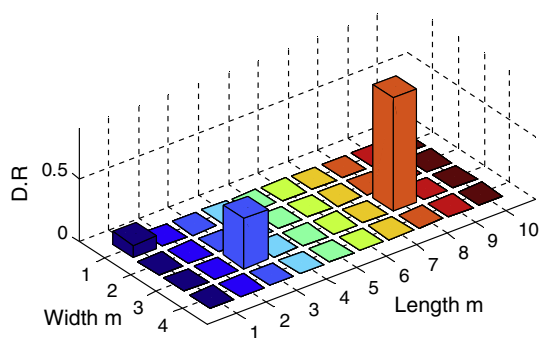


Fig. 11 Damage ratio for combination #5.

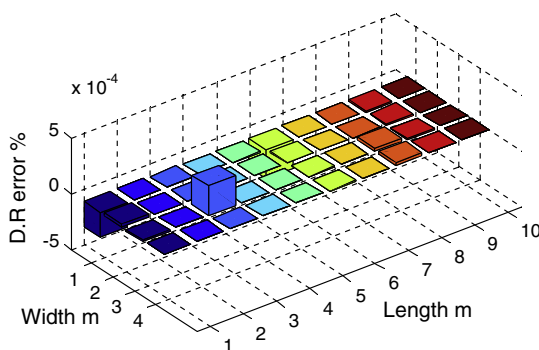


Fig. 12 Damage detection error % for combination #5.

Figs. 10 and 12. It was obtained that the maximum error occurred in element #13 and it was equal to  $2e-4\%$ .

When the error in detecting the damage ratio in the second plate model was compared with that in the first plate model, it was found that this method still acceptable in all plate models.

#### Damage detection of the third model

Figs. 13 and 15 show the damage ratio of the two cases of damages of the third plate model. The detected damage ratios of all cases when a small, moderate and sever damages were occurred in each element individually. The errors in detecting the damage ratio of each case are shown in Figs. 14 and 16. It was shown that the maximum error occurred in case number thirteen and it is equal to  $2.1e-4\%$ . Also, when the error in detecting the damage ratio in this model was compared with

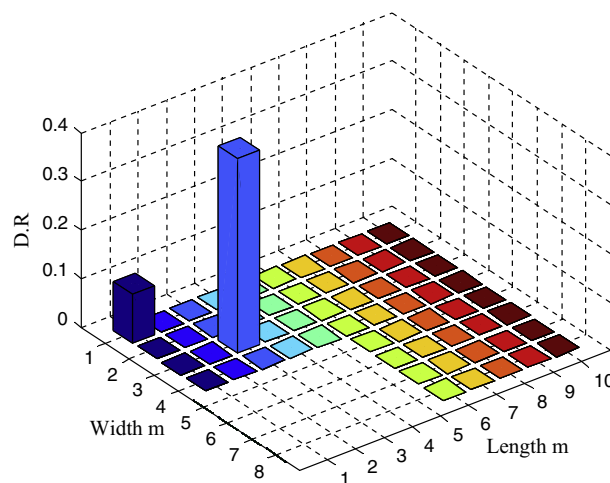


Fig. 13 Damage ratio for combination #6.

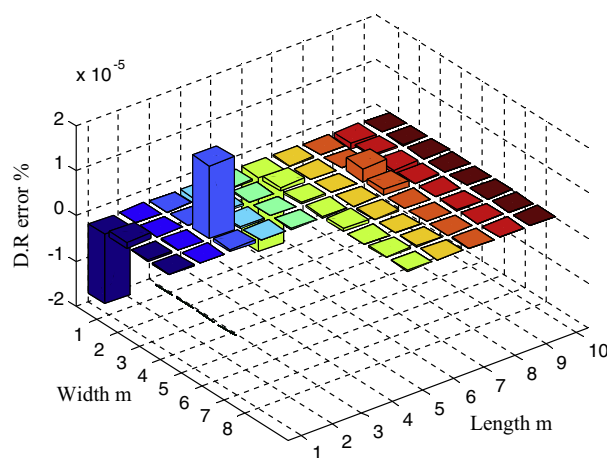


Fig. 14 Damage detection error % for combination #6.

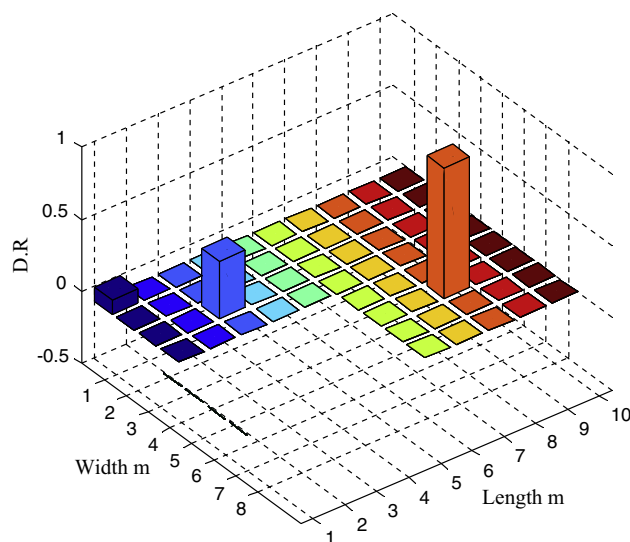
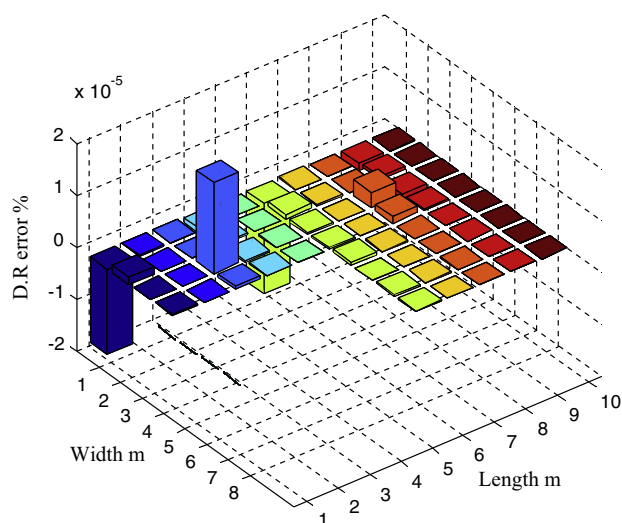


Fig. 15 Damage ratio for combination #7.



**Fig. 16** Damage detection error % for combination #7.

the previous two models, it was found that this method is still acceptable in all plate models.

### Conclusion

Structural damage detection method based on the residual force vector was studied in this paper. Computer program using MatLab was employed to find out the location and degree of damage. The efficiency of the self-made module was examined numerically. Different scenarios for damages applied to three different plate models were simulated.

It was observed that the efficiency of identifying damage in the single plate model is higher than in continuous plate and in L-shape. Moreover, the residual force method was better in identifying minor damage and decreased gradually as in case of severe damage.

Finally, the illustrated numerical examples evidenced that the residual force method can locate single and multiple damage locations accurately in all plate models. The maximum error occurred from this method in identifying the damage did not exceed  $2.7e-4\%$ . As a result, the residual force method is the simplest damage quantification technique which approved to be accurate enough to be used in practical applications.

### Conflict of interest

The author declares that there are no conflict of interests.

### References

- [1] E.V.V. Ramanamurthy, K. Chandrasekaran, Damage detection in composite beam using numerical modal analysis, *Int. J. Design Manuf. Technol.* 2 (2008) 32–43.
- [2] J.C. Chen, J.A. Garba, On-orbit damage assessment for large space structures, *AIAA J.* 26 (1988) 1119–1126.
- [3] D.C. Zimmerman, Structural damage detection using a minimum rank update theory, *J. Vib. Acoust.* 116 (1994) 222–231.
- [4] S.W. Doebling, Minimum-rank optimal update of elemental stiffness parameters for structural damage identification, *AIAA J.* 34 (1996) 2615–2621.
- [5] F.F.M. Leandro, H.L. Rafael, F.F.M. Leticia, A hybrid approach for damage detection of structures under operational conditions, *J. Sound Vib.* 332 (2013) 4241–4260.
- [6] S. Damir, L. Zeljan, V. Damir, An implementation of structural change detection procedure based on experimental and numerical model correlation, *J. Sound Vib.* 331 (2012) 3068–3082.
- [7] D.Y. Chiang, W.Y. Lai, Structural damage detection using the simulated evolution method, *AIAA J.* 37 (1999) 1331–1333.
- [8] C. Mares, C. Surace, An application of genetic algorithms to identify damage in elastic structures, *J. Sound Vib.* 195 (1996) 195–215.
- [9] C. Ratcliffe, Damage detection using a modified Laplacian operator on mode shape data, *J. Sound Vib.* 204 (1997) 505–517.
- [10] K. Pandey, M. Biswas, M.M. Samman, Damage detection from changes in curvature mode shapes, *J. Sound Vib.* 145 (1991) 321–332.
- [11] P. Hajela, F.J. Soeiro, Structural damage detection based on static and modal analysis, *AIAA J.* 28 (1990) 1110–1115.
- [12] S. Chakraverty, R. Jindal, V.K. Agrawal, Effect of non-homogeneity on natural frequencies of vibration of elliptical plates, *Meccanica* 42 (2007) 585–599.
- [13] F.F.M. Leandro, F.F.M. Leticia, K.J. João, Jorge Daniel Riera, Damage detection under ambient vibration by harmony search algorithm, *Expert Syst. Appl.* 39 (2012) 9704–9714.
- [14] B. Titurus, M.I. Friswell, Damage detection using successive parameter subset selections and multiple modal residuals, *Mech. Syst. Signal Process.* 45 (2014) 193–206.
- [15] L.L. Daryl, *A First Course in the Finite Element Method*, fourth ed., Wisconsin, 2007.
- [16] G. Ma, M.L. Eric, Structural damage identification using system dynamic properties, *Comput. Struct.* 83 (2005) 2185–2196.
- [17] A. El-Shihy, H. Soliman, R. Samir, Damage Identification of Structures Using Dynamic Characteristics, PhD Thesis, Zagazig University, 2010.
- [18] R.J. Guyan, Reduction of mass and stiffness matrices, *AIAA J.* 3 (1965) 380.
- [19] F.F.M. Leandro, C.R.M. Ruy, F.F.M. Leticia, Mode shape expansion from data-based system identification procedures, *Mecânica Computacional* 25 (2006) 1593–1602.